

Time-resolved magnetic domain imaging by x-ray photoemission electron microscopy

J. Vogel^{a)}

Laboratoire Louis Néel, CNRS, Boîte Postale 166, F-38042 Grenoble, France

W. Kuch

Max-Planck-Institut für Mikrostrukturphysik, Weinberg 2, D-06120 Halle, Germany

M. Bonfim,^{b)} J. Camarero,^{c)} and Y. Pennec

Laboratoire Louis Néel, CNRS, Boîte Postale 166, F-38042 Grenoble, France

F. Offi, K. Fukumoto, and J. Kirschner

Max-Planck-Institut für Mikrostrukturphysik, Weinberg 2, D-06120 Halle, Germany

A. Fontaine, and S. Pizzini

Laboratoire Louis Néel, CNRS, Boîte Postale 166, F-38042 Grenoble, France

(Received 25 September 2002; accepted 5 February 2003)

X-ray photoemission electron microscopy (X-PEEM) is a powerful imaging technique that can be used to perform element selective magnetic domain imaging on heterogeneous samples with different magnetic layers, like spin valves and tunnel junctions. We have performed nanosecond time-resolved X-PEEM measurements, on the permalloy layer of a Ni₈₀Fe₂₀ (5 nm)/Cu (10 nm)/Co (5 nm) trilayer deposited on Si(111). We used the pump-probe mode, synchronizing a magnetic pulse from a microcoil with the x-ray photon bunches delivered by the BESSY synchrotron in single bunch mode. Images could be acquired during and after the 20 ns long and 80 Oe high field pulses. The nucleation and subsequent growth of reversed domains in the permalloy could be observed, demonstrating the feasibility of element selective and time-resolved domain imaging using X-PEEM. © 2003 American Institute of Physics. [DOI: 10.1063/1.1564876]

Magnetization reversal dynamics at nanosecond time scales is an important subject for many technological applications of magnetic materials. In order to improve the performance of materials for fast magnetic applications, the fundamental understanding of magnetization reversal processes at high speed should be improved. This can be best done using imaging techniques, which allow the direct observation of the local magnetization direction in a sample as a function of time. Up to now, the most successful investigations on microstructured materials have used time-resolved magneto-optical Kerr microscopy.¹⁻³ Femtosecond lasers synchronized with picosecond-long magnetic pulses can be used in pump-probe mode to get access to the temporal evolution of the magnetic domain structure with submicron resolution.¹

Magneto-optical effects analogous to the Kerr effect also exist in the x-ray range. X-ray magnetic circular dichroism (XMCD) is the dependence of x-ray absorption on the relative orientation of the local magnetization and the polarization vector of the circularly polarized light. The element selectivity of this effect, based on the characteristic energy of the absorption edges for each element, has recently been combined with the time structure of synchrotron radiation to separately study the magnetization reversal dynamics of the two ferromagnetic layers of a spin valve system.⁴ Spatial

resolution can be added to this technique by using the magnetic contrast provided by XMCD together with x-ray photoemission electron microscopy (X-PEEM). In X-PEEM, excitation by circularly polarized x-ray synchrotron radiation tuned to atomic absorption edges leads to the emission of secondary electrons at the sample surface, the intensity of which is proportional to the local absorption. These electrons are used to create a magnified image of the sample. In a trilayer system in which two ferromagnetic (FM) layers are separated by a nonmagnetic or an antiferromagnetic spacer layer, the domain patterns in the two FM layers, as well as their correlation and interaction, can be observed separately.⁵⁻⁷

The most performing X-PEEM instruments achieve at present a spatial resolution of 20 nm. Microscopes with an expected resolution down to 2 nm are under construction.⁸ Time resolution is determined by the width of the synchrotron x-ray pulses, which is in the order of some tens of picoseconds for third generation storage rings. Pulse lengths of some tens of femtoseconds are foreseen for fourth generation x-ray sources using x-ray free electron lasers. An exceptional probe of magnetization dynamics of nanostructures will therefore be available when these resolutions will become accessible.

The technical challenges of time-resolved X-PEEM are considerable. A major difficulty for measurements of magnetization dynamics using this technique is the sensitivity of secondary electron trajectories to the applied magnetic field. In order to avoid important displacements of the magnetic

^{a)}Electronic mail: vogel@grenoble.cnrs.fr

^{b)}Present address: Departamento de Engenharia Elétrica, Universidade do Paraná, CEP 81531-990, Curitiba, Brazil.

^{c)}Present address: Departamento Física de la Materia Condensada, Universidad Autónoma de Madrid, 28049 Madrid, Spain.

image in the microscope, the magnetic stray field outside the sample has to be minimized.

We have performed the first nanosecond time-resolved X-PEEM measurements by extending the setup developed for the time-resolved XMCD measurements at the European Synchrotron Radiation Facility.⁴ The measurements were performed on the permalloy layer of a Ni₈₀Fe₂₀ (5 nm)/Cu (10 nm)/Co (5 nm) spin valve-like trilayer deposited on a step-bunched Si(111) substrate. The preparation conditions and the static magnetic properties of the sample have been described in Ref. 9. The terraces of the substrate induce an in-plane uniaxial anisotropy in the magnetic layers, with the easy magnetization axis parallel to the steps. The magnetization dynamics of the two ferromagnetic layers of this sample has already been studied by time-resolved XMCD measurements.⁴ The strength of the “orange-peel” coupling between the soft and the hard magnetic layers induced by the substrate topography decreases going from quasistatic to nanosecond regimes. We tentatively explained this effect supposing that, while propagation of domain walls dominates in the quasistatic regime, nucleation of reversed domains dominates in the nanosecond regime. The coupling in these samples is strongly localized on the steps, and the domain walls have to overcome these strongly coupled regions in order to propagate. Nucleation can take place on all terraces in which case reversal does not require propagation of domain walls across the steps. By using time-resolved X-PEEM, we demonstrate here that nucleation processes dominate the reversal in the nanosecond regime.

The time-resolved X-PEEM measurements were performed at the UE56/2-PGM2 helical undulator beamline of BESSY II in Berlin. The setup of the electrostatic photoelectron emission microscope (Focus IS-PEEM) is identical to that described in previous publications.⁵ The spatial resolution selected for this experiment was of the order of 1 μm , which is well adapted to the study of this magnetic system.

In single bunch mode operation of BESSY, photon bunches are emitted with a repetition rate of 1.25 MHz (800 ns separation between bunches). Measurements were performed in pump-probe mode, by synchronizing nanosecond-short magnetic field pulses with the x-ray photon bunches. Magnetization reversal dynamics was then studied as a function of time, during and after the magnetic pulse, by changing the delay between magnetic and photon pulses.

The sample was set at the inner surface of a double stripline copper coil, made of 12.5- μm -thick Cu foil. The angle of incidence of x rays on the sample was 60° from the surface normal. Magnetic pulses were provided by sending a fast current pulse through a low impedance coaxial cable made of two 12.5- μm -thick and 15 mm wide copper strips connected to the microcoil. The strong currents (up to 30 A) needed to reverse the magnetization of the permalloy layer in dynamic conditions were provided by a current driver¹⁰ based on fast power metal-oxide-semiconductor field effect transistors, located outside the vacuum chamber. At the used repetition rate, up to 50 ns long magnetic pulses with 8 ns rise time could be obtained. The strength of the magnetic field was calculated from the geometry and the current in the coil, with an estimated error of 10%. Due to the deviation of the secondary electrons by the applied magnetic field, images

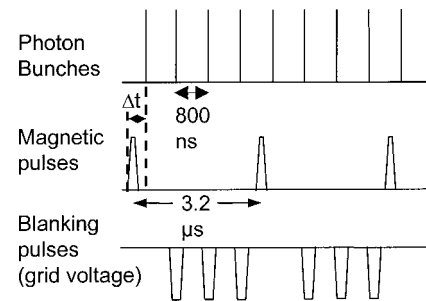


FIG. 1. Photon pulses (top) of about 100 ps length arrive on the sample every 800 ns. A magnetic pulse is given every 3.2 μs (middle), with a width of 20 ns and a delay Δt with respect to one of the photon pulses. For the other three photon pulses, a negative pulse of 80 V and 80 ns width is given to the grid of the PEEM (bottom) to block most of the secondary electrons.

taken during the magnetic field pulse are shifted with respect to the image taken without field. As the field is localized close to the sample, the shift is relatively small (10–15 μm) compared with the field of view (120 μm for this experiment). Correcting this shift might become a serious challenge if a better resolution, and therefore a smaller field of view, needed to be used.

In order to be able to generate sufficiently high magnetic fields, the power dissipation in the microcoil and in the pulse power supply has to be limited. For the measurements presented here a repetition rate of 312.5 kHz was used for the magnetic pulses. This was obtained by passing the 1.25 MHz single-bunch marker signal, used to trigger the power supply, through a 1/4 electronic frequency divider. Only one magnetic pulse was then provided for four photon pulses. Electrons emitted by the photon pulses that are not coupled to a magnetic pulse were blanked out using a retarding field electron energy analyzer,¹¹ located before the imaging unit, acting like a high pass imaging energy filter.¹² Voltage pulses of –80 V height and 80 ns width were provided to the retarding grid of the analyzer by the gated operation of a HP214B pulse generator, while the sample was on ground potential. Electrons emitted with a kinetic energy of less than 80 eV, which constitute more than 95% of the image intensity, are therefore suppressed. The scheme of the synchronization is given in Fig. 1. The delay Δt between photon and magnetic pulse was set using a Stanford Research Systems DG535 delay generator, which also triggered the voltage pulses to the electron analyzer.

The X-PEEM images of the Ni₈₀Fe₂₀/Cu/Co trilayer measured for different delays between field and photon pulses are shown in Fig. 2. The easy magnetization axis is vertical in the figure, and the field pulses are applied parallel to it. The photon energy was tuned to the maximum of the Fe L_3 absorption white line (707 eV), providing sensitivity to the permalloy layer only. The five images were taken with delays of 13, 15, 17, 20, and 22 ns after the maximum of the field pulse. The images, obtained at room temperature, represent the asymmetry (difference divided by sum) of two measurements taken with opposite photon helicity. The contrast is due to the different absorption of regions of the sample having their magnetization parallel and antiparallel to the incoming x-rays direction.

The first positive pulse was used to saturate the permalloy layer, while the dynamics was monitored during the

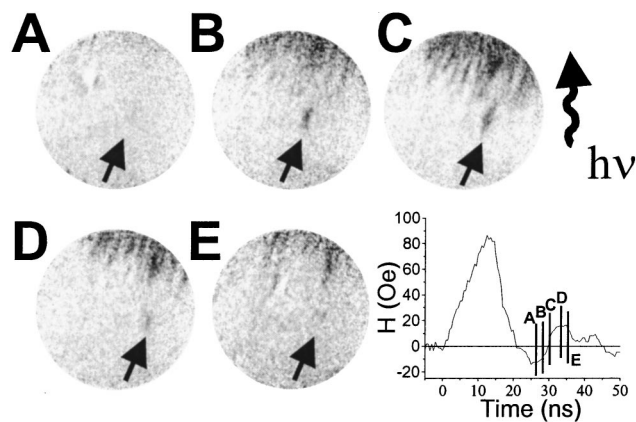


FIG. 2. Magnetic PEEM domain images of a NiFe layer, taken 13, 15, 17, 20, and 22 ns after the maximum of an 80 Oe field pulse. The shape of the pulse as well as the time position with respect to the pulse are given below the images. The arrows indicate a nucleated and subsequently expanding reversed domain. The direction of the incoming photons is also indicated.

negative and subsequent positive overshoot. Acquisition times were of the order of three minutes for each helicity, corresponding to over 100 million of magnetic pulses. The magnetic contrast is limited principally because the nucleation of reversed domains for each magnetic pulse is probably not completely reproducible, but also because the nucleated domains are small with respect to the resolution of the image. In the first image, the nucleation sites which have been generated during the rise of the negative pulse are weakly visible and the clearest of them has been marked with an arrow. In the second and third images the nucleated sites have grown through propagation of the formed domain walls and the contrast becomes larger due to the larger size of the domains. The larger amount of nucleated reverse domains in the top of the image indicates that the field is not completely homogeneous. In the third image, several small, well separated domains can be seen. The domains disappear during the positive overshoot. These results clearly show that for these short pulses the reversal takes place through nucleation of several reversed domains during the rise of the pulse and subsequent propagation of the formed domain walls.

In conclusion, we have shown that time-resolved X-PEEM measurements associated with nanosecond short magnetic field pulses can be used to probe the magnetization reversal dynamics in thin film samples. In the spin-valve

sample studied here, the magnetization reversal of the permalloy layer, which in the quasistatic regime is orange peel coupled to the cobalt layer through a copper layer, is dominated by nucleation processes. This observation supports our explanation for the disappearance of the orange-peel coupling in these samples going from the quasistatic to dynamic regime.⁴

Kerr microscopy allows similar results to be obtained, with comparable spatial and better temporal resolution. The main strength of X-PEEM today is the chemical selectivity. With the improvements in both synchrotron x-ray sources and X-PEEM microscopes, layer selective imaging of magnetization dynamics with picosecond time resolution and spatial resolution down to 2 nm can be foreseen in the near future.

J.C. acknowledges the European Union for a Marie-Curie Fellowship. The authors thank F. Petroff and A. Encinas for sample preparation. Financial support by BMBF (No. 05 KS1EFA6) and EU (BESSY-EC-HPRI Contract No. HPRI-1999-CT-00028) is gratefully acknowledged.

¹B. C. Choi, G. E. Ballentine, M. Belov, W. K. Hiebert, and M. R. Freeman, *Phys. Rev. Lett.* **86**, 728 (2001); B. C. Choi, G. E. Ballentine, M. Belov, and M. R. Freeman, *Phys. Rev. B* **64**, 144418 (2001).

²A. Kirilyuk, J. Ferré, J. Pommier, and D. Renard, *J. Magn. Magn. Mater.* **121**, 536 (1993).

³R. P. Cowburn, J. Ferré, S. J. Gray, and J. A. C. Bland, *Phys. Rev. B* **58**, 11507 (1998).

⁴M. Bonfim, G. Ghiringhelli, F. Montaigne, S. Pizzini, N. B. Brookes, F. Petroff, J. Vogel, J. Camarero, and A. Fontaine, *Phys. Rev. Lett.* **86**, 3646 (2001).

⁵W. Kuch, R. Frömter, J. Gilles, D. Hartmann, Ch. Ziethen, C. M. Schneider, G. Schönhense, W. Swiech, and J. Kirschner, *Surf. Rev. Lett.* **5**, 1241 (1998).

⁶G. Schönhense, *J. Phys.: Condens. Matter* **11**, 9517 (1999).

⁷W. Kuch, X. Gao, and J. Kirschner, *Phys. Rev. B* **65**, 064406 (2002).

⁸R. Fink, M. R. Weiss, E. Umbach, D. Preikszas, H. Rose, R. Spehr, P. Hartel, W. Engel, R. Degenhardt, R. Wichtendahl, H. Kuhlenbeck, W. Erlebach, K. Ihmann, R. Schlögl, H.-J. Freund, A. M. Bradshaw, G. Lilienkamp, T. Schmidt, E. Bauer, and G. Benner, *J. Electron Spectrosc. Relat. Phenom.* **84**, 231 (1997).

⁹A. Encinas, F. Nguyen Van Dau, M. Sussiau, A. Schuhl, and P. Galtier, *Appl. Phys. Lett.* **71**, 3299 (1997).

¹⁰K. Mackay, M. Bonfim, D. Givord, and A. Fontaine, *J. Appl. Phys.* **87**, 1996 (2000).

¹¹Focus Imaging Energy Filter (IEF), Omicron Nanotechnology GmbH.

¹²W. Kuch, L. I. Chelaru, F. Offi, M. Kotsugi, and J. Kirschner, *J. Vac. Sci. Technol. B* **20**, 2543 (2002).